



HARMONIC ANALYSIS ON DIRECTED NETWORKS VIA A BIORTHOGONAL LAPLACIAN CALCULUS FOR NON-NORMAL DIGRAPHS

Chandrasekhar Gokavarapu *Lecturer in Mathematics, Government College (Autonomous), Rajahmundry, A.P., India :: : chandrasekhargokavarapu@gmail.com*

Dr Komala Lakshmi Chinnam *Lecturer in Physics, Government College (Autonomous), Rajahmundry, A.P., India*

Abstract

Spectral graph signal processing is traditionally built on self-adjoint Laplacians, where orthogonal eigenbases yield an energy-preserving Fourier transform and a variational frequency ordering via a real Dirichlet form. Directed networks break self-adjointness: the combinatorial directed Laplacian $L = D_{\text{out}} - A$ is generally non-normal, so eigenvectors are non-orthogonal and classical Parseval identities and Rayleigh-quotient orderings do not apply. This paper develops a Laplacian-centric harmonic analysis for directed graphs that remains exact at the algebraic level while explicitly quantifying the geometric distortion induced by non-normality. We (i) define a Biorthogonal Graph Fourier Transform (BGFT) for L using dual left/right eigenbases and show that vertex energy equals a Gram-metric quadratic form in BGFT coordinates,

(ii) introduce a directed variational semi-norm $TV_G(x) = \|Lx\|_2^2$ and prove sharp two-sided BGFT-domain bounds controlled by singular values of the eigenvector matrix, and (iii) derive sampling and reconstruction guarantees with explicit stability constants that separate sampling-set informativeness from eigenvector geometry. Finally, we provide reproducible simulations comparing a normal directed cycle to perturbed non-normal digraphs and show that filtering and reconstruction robustness track $\kappa(V)$ and the Henrici departure-from-normality $\Delta(L)$, validating the theoretical predictions.

Keywords: Directed graph signal processing, Combinatorial directed Laplacian, Biorthogonal graph Fourier transform, Non-normal matrix analysis, Sampling and reconstruction

2000 MSC: 05C50, 15A18, 94A12, 65F15

1. Introduction

Spectral graph theory is a standard foundation for graph signal processing (GSP), where a graph Fourier transform (GFT) diagonalizes a chosen graph operator and enables filtering, denoising, and sampling on networks [1, 2, 3]. In the undirected case, symmetry yields a self-adjoint Laplacian with a complete orthonormal eigenbasis; the GFT is an isometry and energy, smoothness, and frequency ordering are unified through the Dirichlet quadratic form.

Directed networks are different: the combinatorial directed Laplacian $L = D_{\text{out}} - A$ is typically *non-normal* ($LL^* \neq L^*L$). As a result, eigenvectors are non-orthogonal, the spectral representation is not an isometry, and small perturbations in spectral coefficients can cause large reconstruction errors. This is not a technical nuisance but a structural phenomenon governed by eigenvector geometry and pseudospectral behavior [10, 11].



Positioning and novelty. Existing directed GSP literature often (a) symmetrizes the problem, losing directionality [4], or (b) defines frequency via adjacency/Jordan calculus [5, 6], with additional alternatives including magnetic Laplacians and optimization-based operators [9, 7, 8]. This paper contributes a *Laplacian-variational* directed harmonic analysis that is:

- *Algebraically exact:* analysis/synthesis is exact under diagonalizability, and diagonal filtering is well-defined in BGFT coordinates;
- *Geometrically quantified:* all energy and smoothness identities are stated with explicit Gram-metric and conditioning constants that measure nonnormality-induced distortion;
- *Operational:* sampling and reconstruction statements are given with stability constants that separate sampling-set informativeness from eigenvector non-orthogonality.

Compared with our earlier adjacency-based formulation [12], the present work

(i) uses L to ground frequency in directed variation, (ii) introduces sharp two-sided BGFT bounds for $\|Lx\|_2$ with explicit conditioning constants, and (iii) develops sampling/reconstruction bounds tailored to oblique Laplacian spectral subspaces.

1.1. Contributions

1. **Biorthogonal Laplacian GFT and Gram-metric Parseval law.** We construct the BGFT for the directed Laplacian and prove that vertex energy equals a Gram-metric quadratic form in BGFT coordinates; this yields exact energy bounds in terms of singular values and the condition number $\kappa(V)$.
2. **Directed variation and sharp BGFT-domain smoothness bounds.** We define directed smoothness by $TV_G(x) = \|Lx\|_2^2$ and prove two-sided inequalities that become equalities in the normal case, quantifying when eigenvalue magnitudes behave as directed frequencies.
3. **Sampling/reconstruction with explicit stability constants.** We generalize bandlimited sampling to oblique Laplacian spectral subspaces and give exact recovery and noise sensitivity bounds that separate the roles of $(P_M V_\Omega)^\dagger$ and V_Ω .
4. **Reproducible experiments and quantitative non-normality metrics.** We provide simulations that compute spectra, conditioning, Henrici departure-from-normality, and reconstruction errors on controlled digraph families, demonstrating consistency with theory.

1.2. Organization

Section 2 fixes conventions and non-normality indices. Section 3 defines the BGFT for L and proves energy identities. Section 4 develops directed variation and frequency ordering. Section 5 states sampling and reconstruction results. Section 6 discusses stability mechanisms and practical computation. Section 7 presents experiments, followed by conclusions.



2. Preliminaries

2.1. Directed graphs, adjacency, and out-degree

Let $G = (V, E, w)$ be a directed weighted graph, $|V| = n$, with adjacency $A \in \mathbb{R}^{n \times n}$ given by

$$A_{ij} = w(i, j) \quad \text{if } (i, j) \in E, \quad A_{ij} = 0 \text{ otherwise.}$$

Thus edges are oriented $i \rightarrow j$ and the out-degrees are

$$d_{out_i} = \sum_{j=1}^n A_{ij}, \quad D_{out} = \text{diag}(d_{out_1}, \dots, d_{out_n}).$$

2.2. Combinatorial directed Laplacian

Definition 2.1 (Directed Laplacian). The combinatorial directed Laplacian is $L := D_{out} - A$.

Proposition 2.2 (Row-sum zero). For any directed graph (with any weights), $L\mathbf{1} = 0$.

Proof. The i th entry of $L\mathbf{1}$ equals $d_{out_i} - \sum_j A_{ij} = 0$ by definition.

Remark 2.3 (Non-self-adjointness). If $A \neq A^T$, then typically $L \neq L^T$ and

L is not self-adjoint. Orthogonality of eigenvectors and Rayleigh-quotient variational orderings may fail; this motivates a biorthogonal calculus.

2.3. Asymmetry and non-normality indices

Definition 2.4 (Asymmetry index). For any M , define $\alpha(M) := \|M - M^T\|_F / \|M\|_F$ (with $\alpha(0) = 0$).

Definition 2.5 (Commutator-based departure from normality). For any M , define $\delta(M) := \|MM^* - M^*M\|_F / \|M\|_F^2$ (with $\delta(0) = 0$).

Definition 2.6 (Henrici departure from normality). For any $M \in \mathbb{C}^{n \times n}$ with eigenvalues $\{\lambda_k\}_{k=1}^n$,

$$\Delta(M) := \frac{\|M\|_F^2 - \sum_{k=1}^n |\lambda_k|^2}{n}.$$

$k=1$ Normal matrices satisfy $\Delta(M) = 0$ [10, 11].

3. Biorthogonal Graph Fourier Transform for the directed Laplacian

3.1. Biorthogonal spectral decomposition

We assume L is diagonalizable,¹so

$$L = V \Lambda V^{-1},$$

where $V = [v_1, \dots, v_n]$ contains right eigenvectors ($L v_k = \lambda_k v_k$) and $\Lambda = \text{diag}(\lambda_1, \dots, \lambda_n)$.

¹ Defective cases can be handled with Schur or Jordan calculus; the resulting nonorthogonality effects are typically stronger and are naturally studied through pseudospectra [10].



Define the dual (left) basis via

$$U := (V^{-1})^* \iff U^* = V^{-1}.$$

Then the columns u_k of U satisfy $L^*u_k = \lambda_{-k}u_k$ and biorthogonality holds:

$$u_i^*v_j = \delta_{ij}.$$

3.2. Transform pair

Definition 3.1 (BGFT). For a graph signal $x \in C^n$, its BGFT coefficients are

$$x_b = U^*x = V^{-1}x, \quad x_{bk} = u_k^*x.$$

Definition 3.2 (Inverse BGFT). The inverse BGFT is $x = Vx_b = \sum_{k=1}^n x_{bk}v_k$.

3.3. Gram-metric Parseval identity and energy bounds

Non-orthogonality induces a metric distortion in the spectral domain. Let $M := V^*V$ be the Gram matrix of the right eigenvectors.

Theorem 3.3 (Exact energy identity). For any $x \in C^n$ with BGFT coefficients $x_b = V^{-1}x$,

$$\|x\|_2^2 = x_b^*Mx_b$$

Proof. Since $x = Vx_b$, we have $\|x\|_2^2 = \langle Vx_b, Vx_b \rangle = x_b^*(V^*V)x_b$. \square

Corollary 3.4 (Two-sided Parseval bounds). Let $\sigma_{\min}(V), \sigma_{\max}(V)$ denote the smallest and largest singular values of V . Then

$$\sigma_{\min}^2(V) \|\hat{x}\|_2^2 \leq \|x\|_2^2 \leq \sigma_{\max}^2(V) \|\hat{x}\|_2^2.$$

Equivalently, energy distortion is controlled by $\kappa(V) = \sigma_{\max}(V)/\sigma_{\min}(V)$.

3.4. DC component and mean mode

By Proposition 2.2, $\lambda = 0$ is always an eigenvalue with right eigenvector $\mathbf{1}$. Thus the Laplacian isolates a natural ‘‘DC’’ mode (constant signal), without requiring regularity assumptions that appear in adjacency-based formulations.

4. Directed variation and frequency ordering

4.1. Directed smoothness semi-norm

The quadratic form x^*Lx is generally complex for non-self-adjoint L . Instead, we measure directed variation by the magnitude of the Laplacian response.

Definition 4.1 (Directed total variation).

$$TV_G(x) := \|Lx\|_2^2 = x^*L^*Lx.$$



4.2. BGFT-domain bounds for variation

In undirected GSP, $TV(x)$ equals a weighted sum of $|\lambda_k|^2/x_k^2$. The directed, non-normal case inherits this relation up to sharp conditioning constants.

Theorem 4.2 (Sharp two-sided BGFT variation bounds). *Let $x = Vx_b$ and $L = V\Lambda V^{-1}$. Then*

$$\sigma_{\min}^2(V) \sum_{k=1}^n |\lambda_k/2/x_k^2|^2 \leq \|Lx\|_2^2 \leq \sigma_{\max}^2(V) \sum_{k=1}^n |\lambda_k/2/x_k^2|^2.$$

Proof. We have $Lx = V\Lambda x_b$. For any vector z , $\sigma_{\min}(V)\|z\|_2 \leq \|Vz\|_2 \leq \sigma_{\max}(V)\|z\|_2$. Let $z = \Lambda x_b$ and square the resulting inequalities. \square

Corollary 4.3 (Frequency ordering and tightness). Ordering modes by nondecreasing $|\lambda_k|$ minimizes the upper bound in Theorem 4.2. The interpretation of $|\lambda_k|$ as a directed “frequency” is tight when $\kappa(V)$ is moderate and becomes loose in strongly non-normal regimes.

5. Sampling and reconstruction for L -bandlimited signals

5.1. Bandlimited model

Let $\Omega \subset \{1, \dots, n\}$ be an index set of size K representing low directed frequencies (small $|\lambda_k|$). Define

$$V_{\Omega} := [v_k]_{k \in \Omega} \in \mathbb{C}^{n \times K}, \quad B_{\Omega} := \text{span}(V_{\Omega}).$$

A signal is Ω -bandlimited if $x \in B_{\Omega}$.

5.2. Exact recovery and stability

Let $M \subseteq \{1, \dots, n\}$ be a sampling set of vertices, and let $P_M \in \{0, 1\}^{m \times n}$

be the restriction operator extracting entries indexed by M .

Theorem 5.1 (Exact recovery). *If $x = V_{\Omega}c \in B_{\Omega}$ and $B := P_M V_{\Omega}$ has full column rank K , then x is uniquely determined by $y = P_M x$ and can be recovered by*

$$c_b = B^{\dagger} y, \quad x_b = V_{\Omega} c_b$$

Definition 5.2 (Sampling stability constant). Assuming $\text{rank}(B) = K$, define $\gamma(M, \Omega) := \sigma_{\min}(B) > 0$.

Theorem 5.3 (Noise sensitivity). *If $y = P_M x + \eta$ with noise $\eta \in \mathbb{C}^m$ and x_b is reconstructed by least squares as in Theorem 5.1, then*

$$\|\hat{x} - x\|_2 \leq \|V_{\Omega}\|_2 \frac{\|\eta\|_2}{\gamma(M, \Omega)}.$$

Remark 5.4 (Separation of instability mechanisms). The bound separates



(i) *sampling geometry* via $\gamma(M, \Omega)^{-1}$ and (ii) *eigenvector geometry* via $\|V_\Omega\|_2$ (non-orthogonality/scaling). This separation is specific to the directed, oblique subspace setting.

6. Stability, non-normality, and practical computation

6.1. Reconstruction stability under spectral perturbations

Theorem 6.1 (Coefficient-to-signal amplification). *Let x_b be BGFT coefficients of $x = V x_b$. If coefficients are perturbed to $x_b + \eta$, then*

$$\frac{\|V(\hat{x} + \eta) - V\hat{x}\|_2}{\|x\|_2} \leq \kappa(V) \frac{\|\eta\|_2}{\|\hat{x}\|_2}.$$

Proof. The error is $V \eta$, so $\|V \eta\|_2 \leq \|V\|_2 \|\eta\|_2$. Also $\|x_b\|_2 = \|V^{-1}x\|_2 \leq \|V^{-1}\|_2 \|x\|_2$. Combine and rearrange. \square

6.2. Stable computation of BGFT (recommended)

Computing V^{-1} explicitly can be unstable when $\kappa(V)$ is large. A standard remedy is to use a numerically stable factorization and avoid forming V^{-1} .

Remark 6.2 (Non-normality as a design constraint). In directed filtering and sampling tasks, $\kappa(V)$ and $\Delta(L)$ behave as *intrinsic difficulty indices*. Large values imply that stable spectral filtering may require (i) regularized filter design, (ii) Schur-based spectral methods, or (iii) operator choices other than L for the application at hand.

Algorithm 1 Numerically stable BGFT computation (outline)

Require: Directed Laplacian $L \in \mathbb{R}^{n \times n}$, signal $x \in \mathbb{C}^n$

Ensure: BGFT coefficients x_b

- 1: Optionally scale/balance L to reduce non-normal effects [11]
 - 2: Compute eigen-decomposition $L = V \Lambda V^{-1}$ (or Schur form if needed)
 - 3: Solve the linear system $V x_b = x$ for x_b (do *not* form V^{-1})
 - 4: **return** x_b
-

Table 1: Non-normality and conditioning metrics for the instances used in Figure 1 (computed by make_figures.py with seed 20251221).

Graph	$\kappa(V)$	$\Delta(L)$	$\alpha(L)$	$\delta(L)$
Directed cycle	1	0	1	0
Perturbed cycle	16.80157684	5.981556651	0.4910602974	0.06508077683

7. Experimental validation

7.1. Setup and reproducibility

We compare two digraph families with $n = 20$ nodes:

1. **Directed cycle** (unweighted): $1 \rightarrow 2 \rightarrow \dots \rightarrow n \rightarrow 1$. This L is non-symmetric but normal, yielding an orthogonal eigenbasis.

2. **Perturbed cycle:** starting from the directed cycle, add random directed edges independently with probability $p = 0.2$ and weight $w = 0.8$, increasing non-normality.

All plots in this paper are generated by the included script (`make_figures.py`) with a fixed random seed (see repository note in Data Availability).

7.2. Spectra and non-normality metrics

Figure 1 shows eigenvalues of L in the complex plane for a representative instance of each family.

Table 1 reports the computed non-normality metrics for the same instances (as produced by the script).

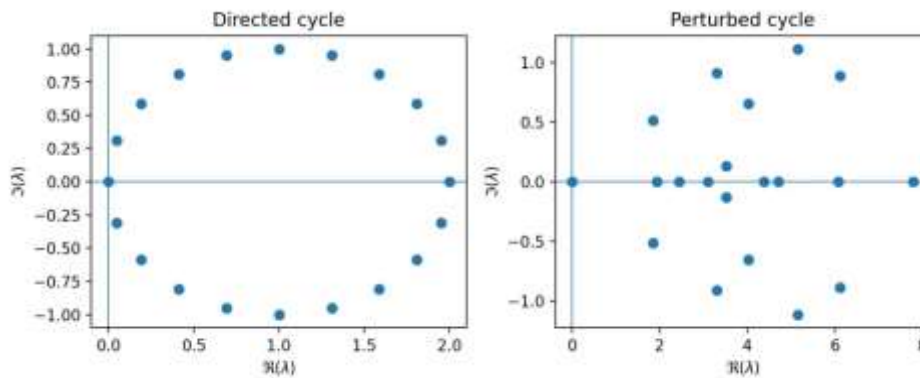


Figure 1: Spectra of the directed Laplacian for a directed cycle (left) and a perturbed cycle (right). Non-normal perturbations visibly deform spectral geometry and typically increase $\kappa(V)$ and $\Delta(L)$.

7.3. Filtering and reconstruction stability

We generate a K -bandlimited signal using the $K = 5$ lowest- $|\lambda|$ modes, add complex Gaussian noise, and reconstruct via ideal low-pass filtering in BGFT coordinates. Figure 2 shows reconstruction error versus input noise level. The observed gap between curves is consistent with Theorem 6.1 and grows with $\kappa(V)$.

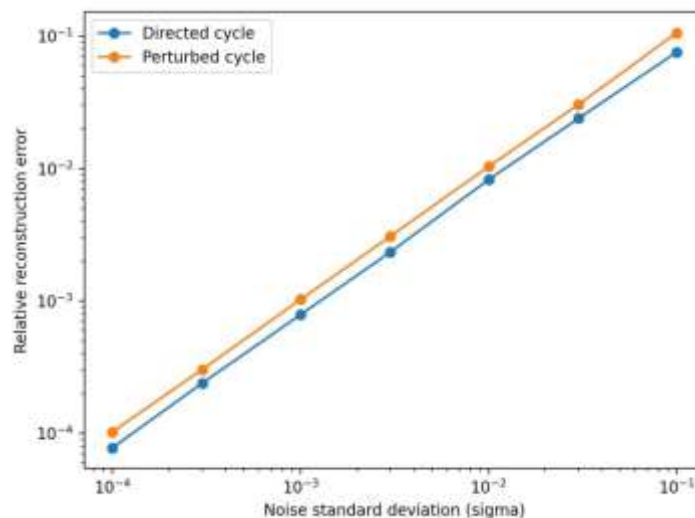


Figure 2: Reconstruction error versus input noise for normal (cycle) and non-normal (perturbed) digraphs. Stronger non-normality typically yields larger amplification in accordance with the conditioning factor $\kappa(V)$.



8. Conclusion

We developed a Laplacian-centric directed harmonic analysis based on the combinatorial directed Laplacian and a biorthogonal spectral calculus. The framework provides exact analysis/synthesis and diagonal filtering while explicitly quantifying metric distortion and instability mechanisms due to nonnormality. Directed variation defined by $\|Lx\|_2$ yields sharp BGFT-domain bounds, and sampling/reconstruction results separate sampling geometry from eigenvector geometry through explicit stability constants. Experiments confirm that filter and reconstruction robustness tracks eigenvector conditioning and departure-from-normality metrics, providing a principled “trust metric” for directed spectral methods.

Acknowledgements

The authors express their gratitude to the Commissioner of Collegiate Education (CCE), Government of Andhra Pradesh, and the Principal of Government College (Autonomous), Rajahmundry, for continued support and encouragement.

Author Contributions

The authors contributed equally in conceptualization, methodology, analysis, software, validation, and writing.

Funding

No external funding was received.

Data Availability Statement

No external datasets were used. The script that generates the figures (make_figures.py) is included for reproducibility; the author will also provide a public repository link upon acceptance.

Conflicts of Interest

The authors declares no conflicts of interest.

References

- [1] D. I. Shuman, S. K. Narang, P. Frossard, A. Ortega, and P. Vandergheynst, “The emerging field of signal processing on graphs,” *IEEE Signal Processing Magazine*, 30(3):83–98, 2013.
- [2] A. Ortega, P. Frossard, J. Kovačević, J. M. F. Moura, and P. Vandergheynst, “Graph signal processing: Overview, challenges, and applications,” *Proceedings of the IEEE*, 106(5):808–828, 2018.
- [3] D. A. Spielman, “Spectral graph theory,” in *Combinatorial Scientific Computing*, U. Naumann and O. Schenk (eds.), Chapman and Hall/CRC, pp. 495–524, 2012.
- [4] F. Chung, “Laplacians and the Cheeger inequality for directed graphs,” *Annals of Combinatorics*, 9(1):1–19, 2005.
- [5] A. Sandryhaila and J. M. F. Moura, “Discrete signal processing on graphs,” *IEEE Transactions on Signal Processing*, 61(7):1644–1656, 2013.
- [6] A. Sandryhaila and J. M. F. Moura, “Discrete signal processing on graphs: Frequency analysis,” *IEEE Transactions on Signal Processing*, 62(12):3042–3054, 2014.
- [7] S. Sardellitti, S. Barbarossa, and P. Di Lorenzo, “On the graph Fourier transform for directed graphs,” *IEEE Journal of Selected Topics in Signal Processing*, 11(6):796–811, 2017.



- [8] A. G. Marques, S. Segarra, and G. Mateos, “Signal processing on directed graphs: The role of edge directionality and the definition of the shift operator,” *IEEE Signal Processing Magazine*, 37(6):99–116, 2020.
- [9] R. Shafipour, A. Khodabakhsh, G. Mateos, and E. Nikolova, “A digraph Fourier transform with generalized translational invariance,” *IEEE Transactions on Signal Processing*, 67(19):4965–4980, 2019.
- [10] L. N. Trefethen and M. Embree, *Spectra and Pseudospectra: The Behavior of Nonnormal Matrices and Operators*, Princeton University Press, 2005.
- [11] N. J. Higham, *Accuracy and Stability of Numerical Algorithms*, 2nd ed., SIAM, 2002.
- [12] C. Gokavarapu, “Asymmetry in spectral graph theory: Harmonic analysis on directed networks via biorthogonal bases (adjacency-operator formulation),” *arXiv preprint*, 2025. (arXiv:2512.11102)